Reaction Paths of Tautomerization between Hydroxypyridines and Pyridones

Noriko Tsuchida and Shinichi Yamabe*

Department of Chemistry, Nara University of Education, Takabatake-cho, Nara 630-8528, Japan

Received: June 25, 2004; In Final Form: November 24, 2004

Tautomerization paths of 2(and 4)-hydroxypyridine (called here HP) to 2(and 4)-pyridone (called here PY) with water molecules were investigated by the use of density functional theory calculations. Potential energies were compared for a number of water molecules. The 2-HP molecule was found to be isomerized most readily and concertedly to the 2-PY one via proton relays with two water molecules. The reaction pattern is invariant even when outer water molecules are added. The 4-HP$(H_2O)_n \rightarrow$ 4-PY$(H_2O)_n$ reaction model did not give small activation energies. However, a reaction of $(4\text{-HP})_2(H_2O)_2 \rightarrow (4\text{-PY})_2(H_2O)_2$ was found to occur readily through a transient ion-pair intermediate. The conversion processes of $(2\text{-PY})_2$ to the tautomerization reacting system were discussed. The hydrogen-bond directionality regulates the tautomerization paths.

I. Introduction

The tautomeric equilibria both between 2-hydroxypyridine-(2-HP) and 2-pyridone(2-PY) and between 4-hydroxypyridine-(4-HP) and 4-pyridone(4-PY) have been extensively studied.[1−3] While in gas phase or in nonpolar solvent the 2-HP (and 4-HP) form is dominant, in aqueous solution or in polar solevnt 2-PY (and 4-PY) form predominates.[1b,1c,4] The change in equilibrium constants may be attributed to dimerization of the 2-PY form and to the larger stability of solvent···pyridone complexes.[5]

For the species in Scheme 1a, there is an interconversion in a self-associated dimer (Scheme 2).

In the crystalline state, the $(2\text{-PY})_2$ form is predominant.[6] Experimental studies showed that a proton transfer with one or more water molecules is the more important mechanism than the transfer in Scheme 2.[5c] There have been many theoretical studies of the tautomerism.[7] Field and Hillier investigated the paths of two transfers (in Scheme 2 and one- and two-water assisted reactions in Scheme 1a) with CISD/3-21G//RHF/3-21G.[7e] A proton relay in the 2-HP (or 2-PY) and water dimer was computed to be the best reaction pattern. The 2-HP/2-PY tautomerism, both for the isolated isomers and for the possible dimers, has been studied by various authors.[8−10] The 2-PY/2-PY homo−dimer complex was reported to be the most stable.[10a] Experimental data on the geometry of the most favorable dimer as well as low frequencies of the 2-PY/2-PY and 2-HP/2-PY dimers gives a basis to rationalize the calculation methods used.[8c,9a,9d−f,9h,10] Twelve isomeric dimer geometries composed of 4-HP and 4-PY were calculated, and the hydrogen bond energies showed a clear preference for 4-PY-containing dimers.[11]

Despite accumulation of those experimental and theoretical studies, systematic simulations of tautomerization reactions in aqueous media (Scheme 1) has not been made. Particular interest is in the way of the proton shift in Scheme 1b. In this work, proton-relay reactions involving water molecules were investigated by B3LYP/6-31G* SCRF calculations. The best path was sought in terms of the Gibbs activation free energies.

II. Calculation Methods

The geometries of HP, PY, $(HP)_2$, $(PY)_2$ and their water added models (e.g., 2-HP$(H_2O)_n$, $n = 1-3$ and 8) were determined by density functional theory calculations. B3LYP/6-31G* methods[12] were used for geometry optimizations. The solvent effect was taken into account by Onsager's self-consistenet field with the dielectric constant = 78.39 (water).[13] B3LYP seems to be a suitable method for the present large systems, because it includes the electron correlation effect to some extent.

Transition states (TSs) were characterized by vibrational analyses, which checked whether the obtained geometries have single imaginary frequencies ($\nu^{\ddagger}$s). From TSs, reaction paths were traced by the IRC (intrinsic reaction coordinate) method[14] to confirm that reactants and products are hydroxypyridine and pyridone forms, respectively. All the calculations were carried out using the GAUSSIAN 98[15] program package installed on

SCHEME 1: Tautomerism of Hydroxypyridines and Pyridones

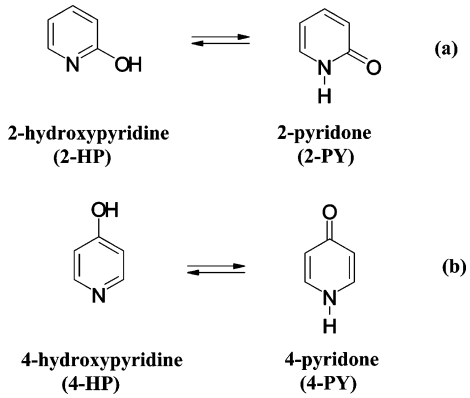

SCHEME 2: Symmetric Dimers Based on Two Intermolecular Hydrogen Bonds

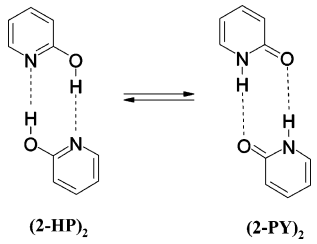

10.1021/jp040451w CCC: $30.25
Published on Web 02/12/2005

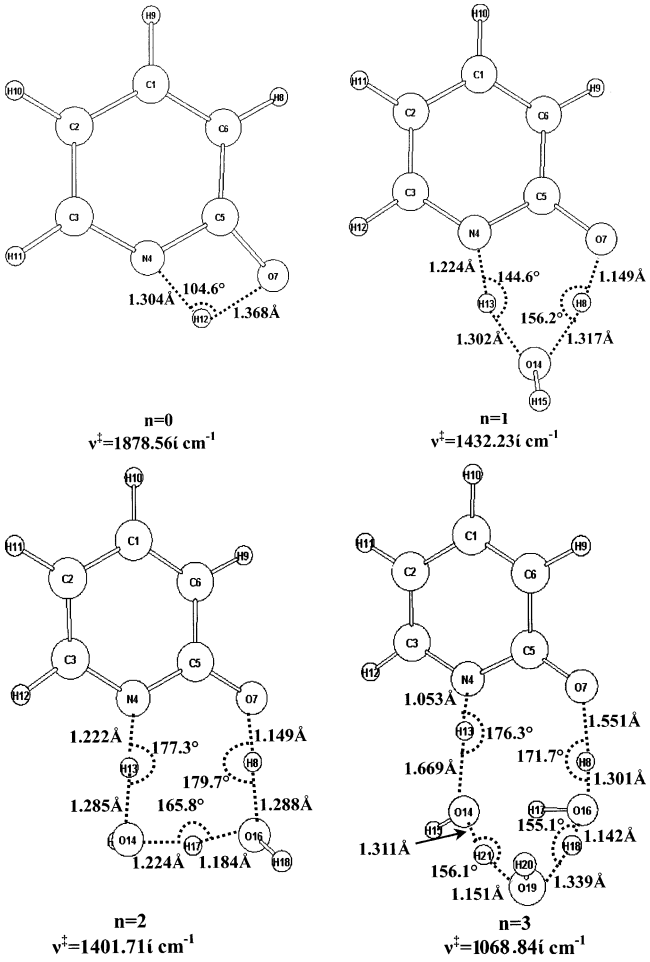

Figure 1. Transition-state (TS) geometries of the tautomerization between 2-HP$(H_2O)_n$ and 2-PY$(H_2O)_n$. Empty circles stand for hydrogen atoms. Sole imaginary frequencies($\nu^{\ddagger}$s) verify that the obtained geometries are correctly at the saddle point. More detailed data of TSs along with the results of 2-HP$(H_2O)_n$ and 2-PY$(H_2O)_n$ after IRC searches are given in figures S2 ($n = 0$), S3 ($n = 1$), S4 ($n = 2$), and S5 ($n = 3$).

Compaq ES 40 at the Information Processing Center (Nara University of Education).

III. Calculated Results and Discussions

Reactions of 2-HP → 2-PY. In this subsection, the tautomerizaton paths of 2-hydroxypyridine (2-HP) to 2-pyridone (2-PY) were traced. Figure 1 shows transition state (TS) geometries of those paths. Water molecules ($n > 0$) are involved so as to give strainless proton relays. Reactant and product geometries corresponding to the TS ones are shown in Figures S2 ($n = 0$), S3 ($n = 1$), S4 ($n = 2$), and S5 ($n = 3$) of the Supporting Information. As n grows larger, the hydrogen-bond directionality becomes better, and O···H···O and N···H···O angles approach 180°. However, the $n = 3$ TS contains a new strain of dihedral angles. As far as the geometries are concerned, the $n = 2$ TS seems to be the best model. The shape of the proton-relay route is close to that of the hydrogen-bond region in scheme 2. The changes in Gibbs free energies along the tautomerization paths are exhibited in Figure 2. In accord with the geometric results in Figure 1, the $n = 2$ model has the lowest energy change. Thus, the 2-HP$(H_2O)_2$ → 2-PY$(H_2O)_2$ reaction is the best to describe the tautomerization. The result was assessed by the use of a larger cluster model, 2-HP$(H_2O)_{2+6}$ → 2-PY$(H_2O)_{2+6}$ (Scheme 3).

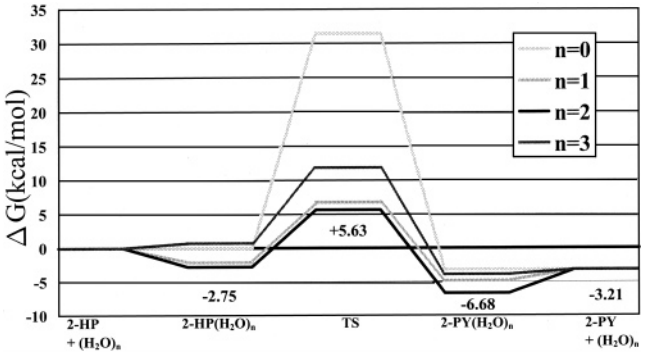

Figure 2. Changes of Gibbs free energies for tautomerization reactions of 2-HP$(H_2O)_n$ → 2-PY $(H_2O)_n$.

SCHEME 3: Picture of the Initial Geometry to Seek the TS One of n=2+6

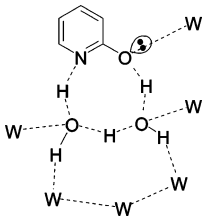

W_s stand for outer water molecules.

If the reaction region of $n = 2$ were broken by addition of six outer water molecules, the $n = 2$ model could not be characterized as the basic part of the tautomerization. Figure 3 shows geometries of 2-HP$(H_2O)_8$ → TS → 2-PY$(H_2O)_8$. The proton-relay shape of $n = 8$ is found to be very similar to that of $n = 2$. Thus, $n = 8$ may be regarded as $n = 2+6$, and the $(H_2O)_2$ containing tautomerization path of (2-HP → 2-PY) is thought to be meaningful.

In Scheme 2 (Introduction), the C_{2h}-symmetry dimers of $(2\text{-HP})_2$ and $(2\text{-PY})_2$ have been shown. The conversion process of the $(2\text{-HP})_2 \leftrightarrows (2\text{-PY})_2$ equilibrium to that of 2-HP$(H_2O)_2 \leftrightarrows$ 2-PY$(H_2O)_2$ in $n = 2$ TS of Figure 1 was investigated. The 2-HP dimer was found to be insusceptible to geometric deformation by association of water clusters, and the C_{2h} geometry of the $(2\text{-HP})_2$ fragment in $(2\text{-HP})_2(H_2O)_n$ is retained by optimizations. On the other hand, the $(2\text{-PY})_2$ geometry is susceptible to the puckering deformation along the first vibrational mode ($\nu_1 = 18.36$ cm^{-1}) via the $(H_2O)_4$ association (Scheme 4b and Figure 6S(b) in Supporting Information). The deformation leads to instability of the cyclic dimer of $(2\text{-PY})_2$. In fact, the NH···O═C distances (= 1.908 Å and 1.948 Å) in Scheme 4b are larger than those (= 1.797 Å and 1.798 Å) in Scheme 4a. Also, the stability rank by Gibbs free energies is c > a > b in Scheme 4. Thus, the cyclic dimer, $(2\text{-PY})_2$ in Scheme 2, is converted to 2-PY$(H_2O)_2$ via the water associated and puckered form dimer, Scheme 4b.

Reactions of 4-HP → 4-PY. In the previous subsection, the water dimer has been found to work for the effective proton relay in the tautomerization. The relay pattern might be extended to the tautomerization as 4-HP$(H_2O)_n$ → 4-PY$(H_2O)_n$. The $n =$ 0 and 1 reaction paths were computed to be absent, which is evident in view of the large distance of 1 and 4 (para) positions of OH and N. The $n = 2$ model appears to be present as the upper side of Figure 4 shows. However, during the geometry optimization, the water dimer became linked merely to the OH group of 4-PY. The $n > 2$ models are needed to construct hydrogen-bond networks. TS geometries of $n = 3-6$ are shown

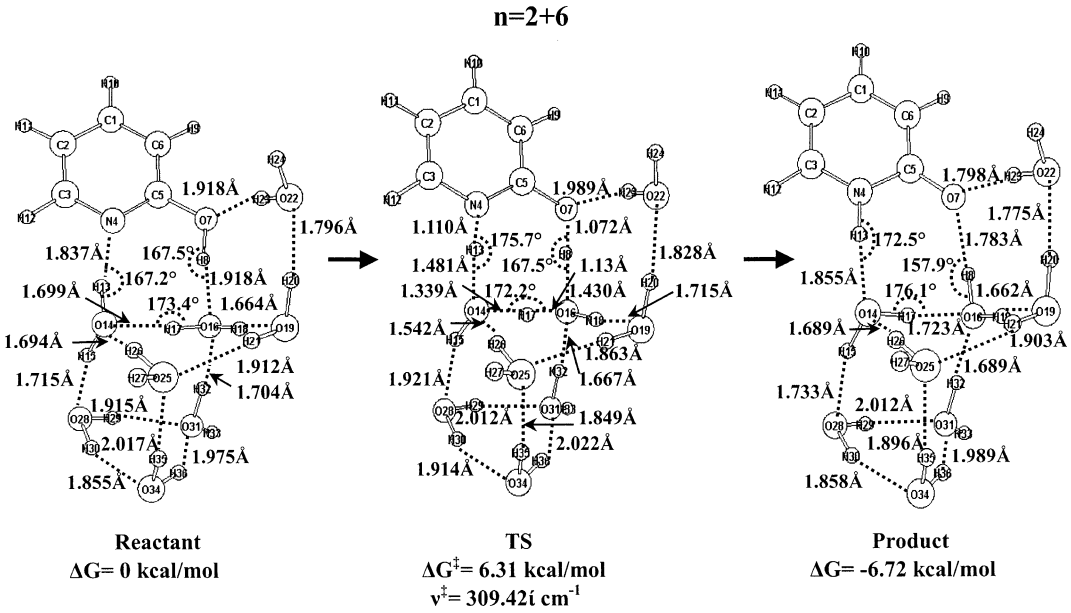

Figure 3. A tautomerization of 2-HP$(H_2O)_8$ → 2-PY$(H_2O)_8$. Among eight water molecules, two are reactants and six are catalysts.

SCHEME 4: Separation Process of the 2-HP Dimer with Two Water Dimers

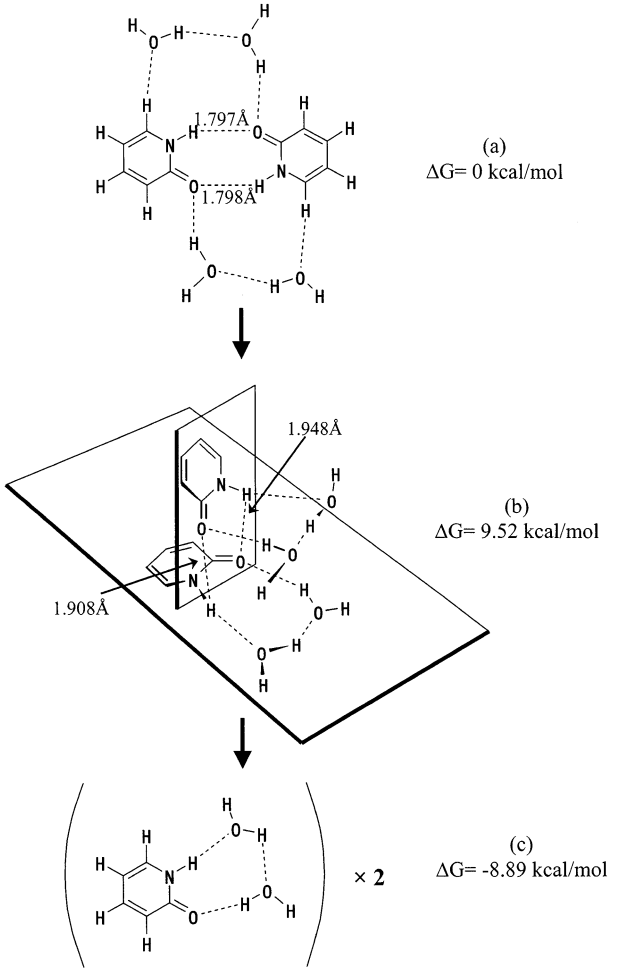

ΔG is the relative free energy. The optimized geometries are exhibited in Figure S6 (Supporting Information).

in Figure 5. Their detailed reaction paths are exhibited in Figures S7 ($n = 3$), S8($n = 4$), S9($n = 5$), and S10 ($n = 6$). As n grows larger, the proton relay circuit becomes more strainless and $\Delta G^{\ddagger}$ becomes smaller. $\Delta G^{\ddagger}$ is the difference of Gibbs free energies between 4-HP$(H_2O)_n$ (the hydrogen bonded precursors in the left sides of Figures S7-S10) and TS. However, association of $(H_2O)_5$ or $(H_2O)_6$ to the substrate, 4-HP, is entropically very difficult. If a drastically small $\Delta G^{\ddagger}$ value was obtained, the 4-HP$(H_2O)_5$ or 4-HP$(H_2O)_6$ model would be meaningful. However, the $\Delta G^{\ddagger}$ values are larger than $\Delta G^{\ddagger} = 8.38$ (= 5.63−(−2.75)) kcal/mol in Figure 2. The proton-relay paths in Figure

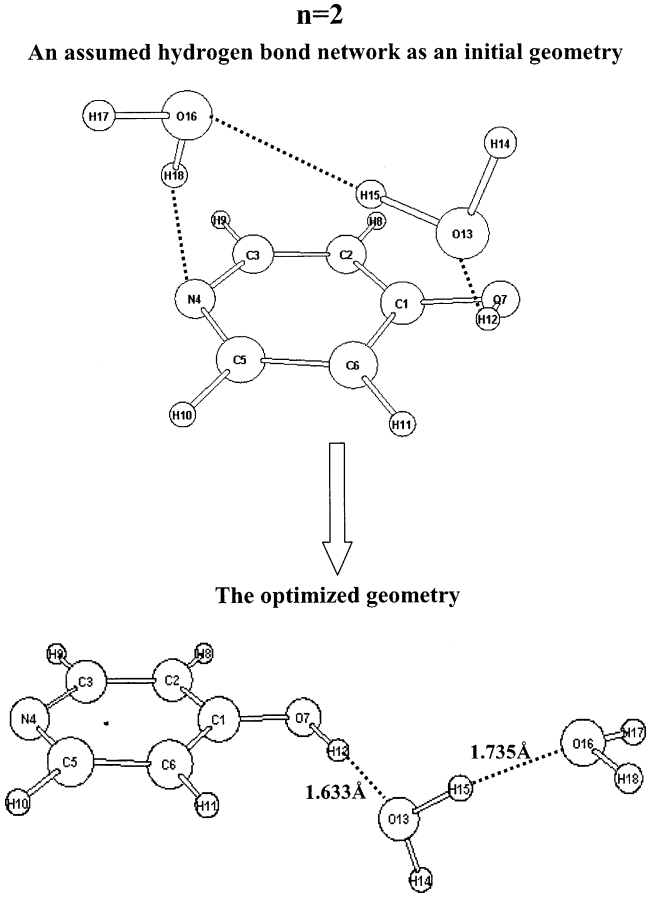

Figure 4. Geometries of 4-HP$(H_2O)_2$ before and after the optimization. A hydrogen bond network cannot be formed in the 4-HP$(H_2O)_2$ model.

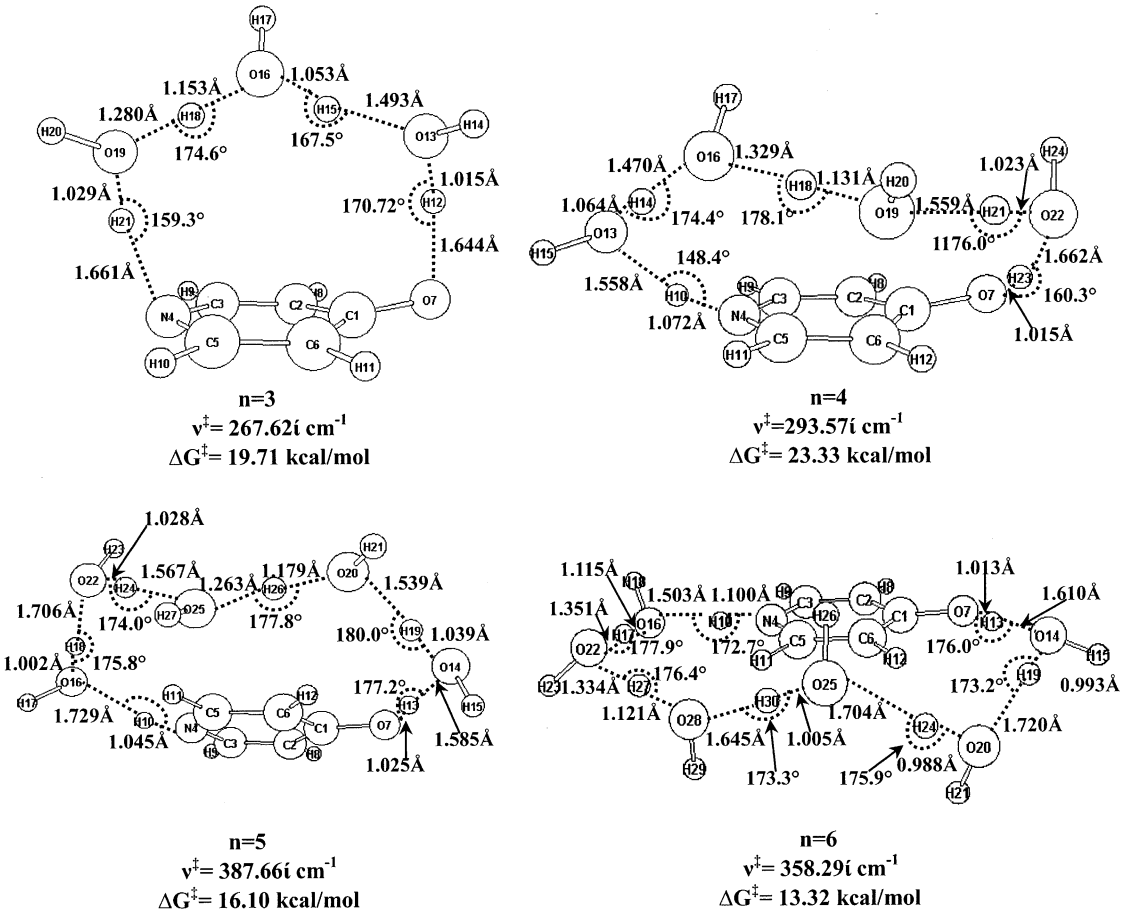

Figure 5. TS geometries of the tautomerization between 4-HP$(H_2O)_n$ and 4-PY$(H_2O)_n$. The $n < 3$ models cannot be constructed owing to the too small cluster of $(H_2O)_n$ to fit the 1 and 4 positions of the substrate.

SCHEME 5: Permanent Dipole−Dipole Interaction in the van der Waals Force, Which Gives 2.17 kcal/mol Stabilizing Energy

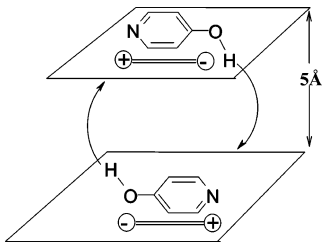

5 are thought to be unlikely. The (4-HP → 4-PY) isomerization route must be reconsidered.

The free 4-HP molecule was computed to have a large dipole moment, 3.48 D. The polar molecule may be stabilized substantially in the antiparallel stacking by the permanent dipole−dipole interaction. For instance, at an assumed large layer distance = 5 Å, the dipole−dipole interaction gives −2.17 kcal/mol stabilizing energy (T = 300 K, Scheme 5).[16]

The antiparallel alignment would cause ready mutual proton transmittal as two arrows in Scheme 5 indicate. According to the alignment, an initial geometry was modeled as is shown in the upper side of Figure 6. The geometry was transformed, however, to the linear hydrogen bonded one and the stacking orientation could not be obtained.[17] Auxiliary water molecules are needed to ensure the antiparallel stacking (Scheme 6).

The numbers of n and m were changed systematically. The computed results of the tautomerization of (4-HP)$_2(H_2O)_n$ → (4-PY)$_2(H_2O)_n$ are shown in Figures S11 (m=n=1), 7(m=1 and n=2), S12(m=2 and n=3), S13 (m=2 and n=4), and S14 (m=3 and n=5). Figures S*s* are in Supporting Information. Every reaction path was found to have an ion pair intermediate (Int, Scheme 7).

SCHEME 6: Proton-Relay Reactions via $(H_2O)_m$ and $(H_2O)_{n-m}$ Cluster

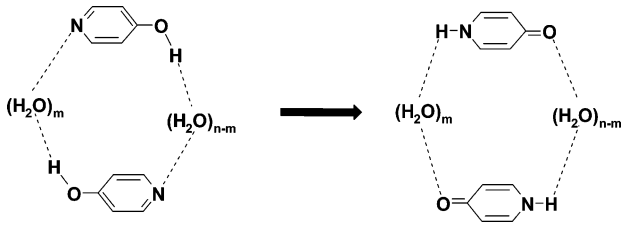

SCHEME 7: Transient Ion-Pair Intermediate (Int) during the Mutual Proton Relays for the Tautomerization

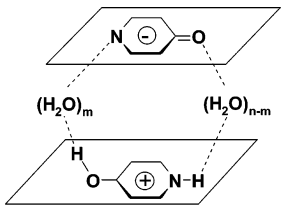

Int

Every reaction is described as the process (4-HP)$_2(H_2O)_n$ → TS1 → Int →TS2 → (4-PY)$_2(H_2O)_n$. The energy of Int is similar to that of TS1 or TS2, and Int is a very transient and unstable intermediate.

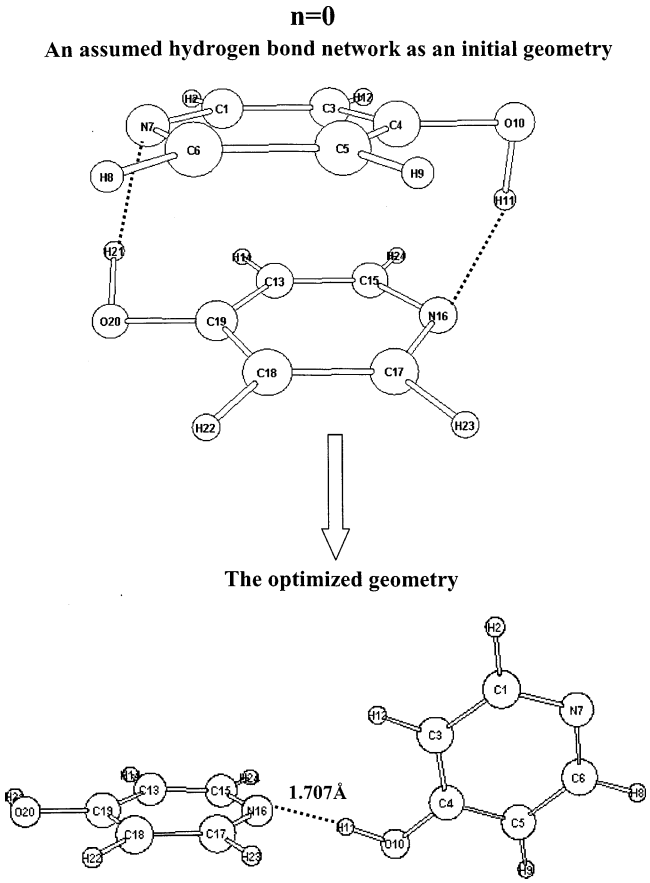

Figure 6. Geometries of $(4\text{-HP})_2$. The upper one is an anti-parallel stacking, which gives stability of the dipole−dipole interaction. After the geometry optimization, the stacking conformation is converted to the linear alignment shown below.

Gibbs activation energies ($\Delta G^{\ddagger}$) are compared in Table 1. Two models, ($n = 2$, $m = 1$) and ($n = 4$, $m = 2$) have small $\Delta G^{\ddagger}$ values ~9 kcal/mol. Both involve symmetric geometries of $(4\text{-HP})_2(H_2O)_n$ and $(4\text{-PY})_2(H_2O)_n$. In view of the energies in Table 1, one may see that the size extension does not improve (lower) the energies. Introduction of excessive water molecules to the reaction models gives rise to their entropic destabilization. When two outer water molecules are added to the ($n = 2$, $m = 1$) model, free activation energies become smaller, $\Delta G^{\ddagger}$(TS1) = 4.55 kcal/mol and $\Delta G^{\ddagger}$(TS2) = 1.49 kcal/mol ($n = 4$, $m = 1+1$) in Figure S16. Thus, the ($n = 2$, $m = 1$) model is the minimum and optimal one, which is shown in Figure 7. In the Figure, the right-sided and the first proton (H11 and H27) relay takes place via TS1 leading to Int. From Int, the left-sided and the second (H21 and H29) relay via TS2 leads to the product, $(4\text{-PY})_2(H_2O)_2$. The antiparallel stacking of two 4-HP molecules sandwiches two water molecules ($m = 1$ and $n = 2$), which results in ready tautomerization to two 4-PY ones.

TABLE 1: Gibbs Free Activation Energies (kcal/mol) of the Stepwise Path, $(4\text{-HP})_2(H_2O)_n \rightarrow$ TS1 $\rightarrow$ Int $\rightarrow$ TS2 $\rightarrow$ $(4\text{-PY})_2(H_2O)_n$, Relative to the Energy of $(4\text{-HP})_2(H_2O)_n$

n	m	$\Delta G^{\ddagger}$(TS1) kcal/mol	$\Delta G^{\ddagger}$(TS2) kcal/mol	figure no.
1	1	11.62	12.93	S11
2	1	9.24	9.18	7
3	2	11.32	10.36	S12
4	2	9.13	8.66	S13
5	3	9.95	11.82	S14
4	1 + 1	4.55	1.49	S16

[a] The integer m is defined in Scheme 6, and the shape of Int is shown in Scheme 7. Figure S*s* are in Supporting Information.

For the chain of $(4\text{-HP})_n$, water molecules invade the interlayer space. The axial new hydrogen bonds supported by two water molecules would take off the stacked 4-HP dimer (Scheme 8).

IV. Concluding Remarks

In this work, tautomerization paths of (2-HP → 2-PY) and (4-HP → 4-PY) through proton relays have been investigated computationally. For 2-HP, the water dimer has afforded a

SCHEME 8: Model of Hydrogen Bonded Polymers of 4-HP and Water (w) Invasion to Form the Tautomerization Path

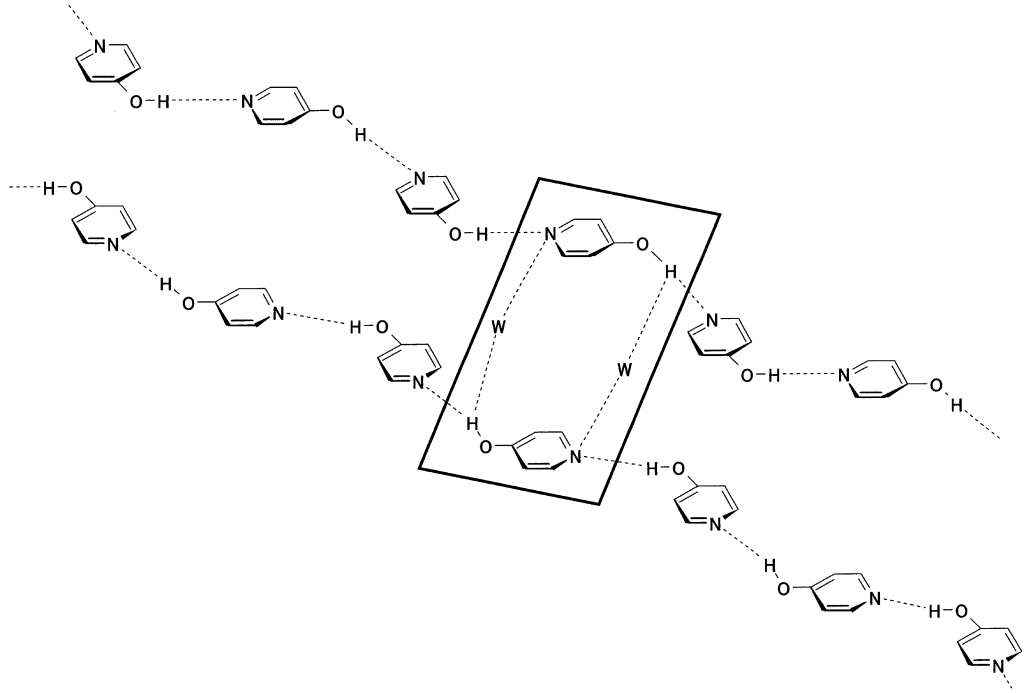

The linear 4-HP cluster is more stable than the 4-PY one.

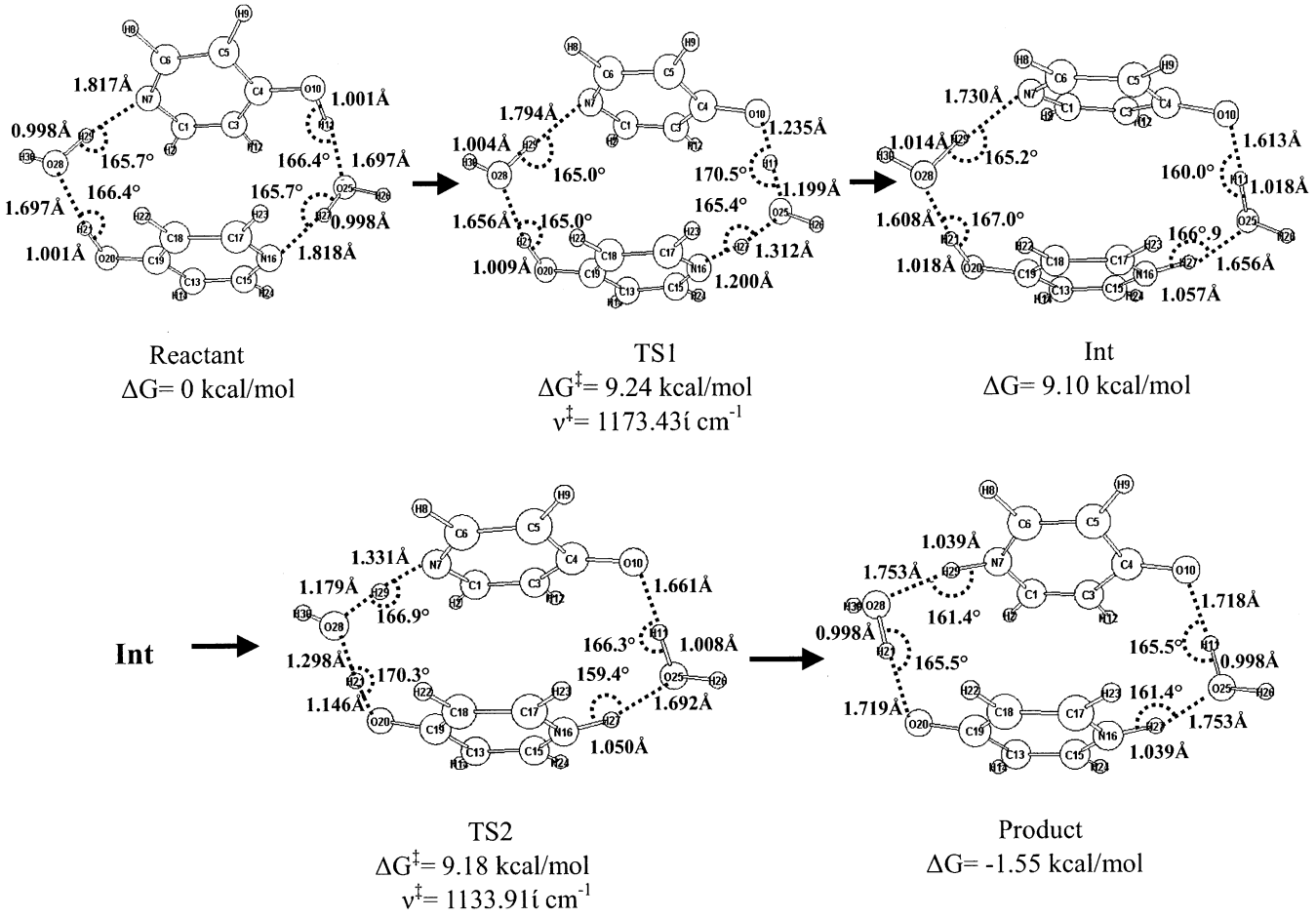

Figure 7. Reaction path between $(4\text{-HP})_2$ and $(4\text{-PY})_2$ with two water molecules ($n = 2$, $m = 1$). "Int" denotes an ion-pair intermediate.

SCHEME 9: Summary of the Present Calculations for Two Tautomerizations

The most favorable path, 2-HP$(H_2O)_2$ ⇆ 2-PY$(H_2O)_2$

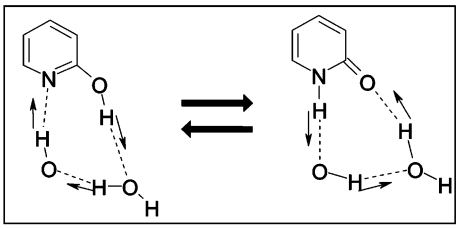

The most favorable path, $(4\text{-HP})_2(H_2O)_2$ ⇆ $(4\text{-PY})_2(H_2O)_2$

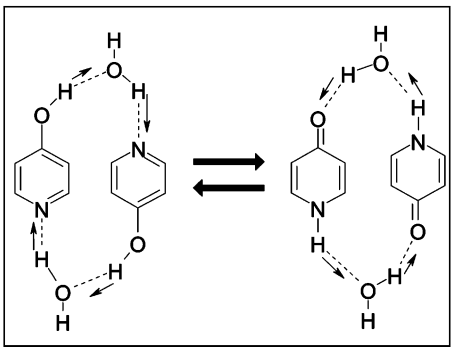

reasonable proton relay path. For 4-HP, also two water molecules have the role of proton donors and acceptors. There is a crucial difference between 2-HP and 4-HP reactions. The monomer of 2-HP is involved in the tautomerization. The 2-PY monomer is evolved from the dimer via the water association. In contrast to the reaction of 2-HP$(H_2O)_2$, the dimer of 4-HP undergoes the mutual proton relays via an unstable ion-pair intermediate (Int). The contrast is shown in Scheme 9.

Acknowledgment. The authors thank Miss Aki Kitamori for her partial assistance in DFT calculations.

Supporting Information Available: Figure S1 shows geometries of monomers of 2(4)-HPs and 2(4)-PYs. Figure S6 shows those of $(2\text{-PY})_2(H_2O)_4$ and 2-PY$(H_2O)_2$. Figures S2−S5 and S7−S16 display reaction paths of tautomerizations and isomerizations. This material is available free of charge via the Internet://pubs.acs.org.

References and Notes

(1) (a) Beak, P.; Fry, F. S.; Steele, F. *J. Am. Chem. Soc.* **1976**, *98*, 171. (b) Beak, P. *Acc. Chem. Res.* **1977**, *10*, 186. (c) Beak, P.; Convington, J. B. *J. Am. Chem. Soc.* **1978**, *100*, 3961. (d) Beak, P.; Convington, J. B.; Smith, S. G. *J. Am. Chem. Soc.* **1976**, *98*, 8284.

(2) (a) Elguero, J.; Marzin, C.; Katritzky, A. R.; Linda, P. *The Tautomerism of Heterocycles*; Katrirzky, A. R., Boulton, A. J., Eds.; Academic Press: New York, 1976; Suppl. No.1. (b) Gordon, A.; Katritzky, A. R. *Tetrahedron Lett.* **1968**, 2767. (c) Frank, J.; Katritzky, A. R. *J. Chem. Soc., Perkin Trans. 2* **1976**, 1428.

(3) (a) Brown, R. S.; Tse, A.; Vedras, J. C. *J. Am. Chem. Soc.* **1980**, *102*, 1174. (b) Guimon, C.; Garrabe, G.; Pfister-Guillouzo, G. *Tetrahedron Lett.* **1979**, 2585. (c) Nowak, M. j.; Lapinski, L.; Rostkowska, H.; Les, A.; Adamowicz, L. *J. Phys. Chem.* **1990**, *94*, 7406. (d) Nowak, M. j.; Lapinski, L.; Fulara, J.; Les, A.; Adamowicz, L. *J. Phys. Chem.* **1992**, *96*, 1562, 6250.

(4) Suradi, S.; El Saiad, N.; Pilcher, G.; Skinner, H. A. *J. Chem. Theromodyn.* **1982**, *14*, 45.

(5) (a) Bensaude, O.; Dreyfus, M.; Dodin, G.; Dubois, J. E. *J. Am. Chem. Soc.* **1977**, *99*, 4438. (b) Bensaude, O.; Chevrier, M.; Dubois, J. E. *J. Am. Chem. Soc.* **1978**, *100*, 7055. (c) Bensaude, O.; Chevrier, M.; Dubois, J. E. *J. Am. Chem. Soc.* **1979**, *101*, 2423. (d) Chevrier, M.; Guillerez, J.; Dubois, J. E. *J. Chem. Soc., Perkin Trans. 2* **1983**, 979.

(6) (a) Penfold, B. *Acta Crystallogr.* **1953**, *6*, 591. (b) Wheeler, G. L.; Ammon, H. L. *Acta Crystallogr.* **1974**, *B30*, 680. (c) Slanina, Z.; Le, A.; Adamowicz, L. *J. Mol. Struct.* **1992**, *257*, 491.

(7) (a) Fabian, W. M. F. *J. Comput. Chem.* **1991**, *12*, 17. (b) Moreno, M.; Miller, W. H. *Chem. Phys. Lett.* **1990**, *171*, 475. (c) Schlegel, H. B.; Gund, P.; Fluder, E. M. *J. Am. Chem. Soc.* **1982**, *104*, 5347. (d) Scanlan, M. j.; Hillier, I. H.; MacDowell, A. A. *J. Am. Chem. Soc.* **1983**, *105*, 3568. (e) Field, M. J.; Hillier, I. H. *J. Chem. Soc., Perkin Trans. 2* **1987**, 617. (f) Perchment, O. G.; Burton, N. A.; Hillier, I. H.; Vincent, M. A. *J. Chem. Soc., Perkin Trans. 2* **1993**, 861. (g) Young, P.; Green, D. V. S.; Hillier, I. H.; Burton, N. A. *Mol. Phys.* **1993**, *80*, 503. (h) Hall, R. J.; Burton, N. A.; Hillier, I. H.; Young, P. E. *Chem. Phys. Lett.* **1994**, *220*, 129. (i) Cieplak, P.; Bash, P.; Singh, U. C.; Kollman, P. A. *J. Am. Chem. Soc.* **1987**, *109*, 6283. (j) Wong, M. W.; Wiberg, K. B.; Frisch, M. J. *J. Am. Chem. Soc.* **1992**, *114*, 1645. (k) Cramer, C. J.; Truhlar, D. G. *J. Am. Chem. Soc.* **1991**, *113*, 8552. (l) Cramer, C. J.; Truhlar, D. G. *J. Comput.-Aided Mol. Design.* **1992**, *6*, 629. (m) La Manna, G. *J. Mol. Struct. (THEOCHEM)* **1981**, *85*, 389. (n) La Manna, G.; Vwnuti, E. *J. Compt. Chem.* **1982**, *3*, 593. (o) Gao, J.; Shao, L. *J. Phys. Chem.* **1994**, *98*, 13772. (p) Del Bene, J. E. *J. Phys. Chem.* **1994**, *98*, 5902. (q) Wang, J.; Boyd R. J. *J. Phys. Chem.* **1996**, *100*, 16141. (r) Hug, F.; Yu, J. Q. *J. Mol. Model.* **2002**, *8*, 81. (s) Maran, U.; Krleson, M.; Katritzky, A. R. *Int. J. Quantum Chem. Quantum Bio. Symp.* **1996**, *23*, 1765.

(8) (a) Parchment, O. G.; Burton, N. A.; Hillier, I. H. *Chem. Phys. Lett.* **1993**, *203*, 46. (b) Barone, V.; Adamo, C. *J. Phys. Chem.* **1995**, *99*, 15062. (c) Dkhissi, A.; Ramaekers, R.; Houben, L.; Adamowicz, L.; Maes, G. *Chem. Phys. Lett.* **2000**, *331*, 553. (d) Maris, A.; Ottaviani, P.; Caminati, W. *Chem. Phys. Lett.* **2002**, *360*, 155.

(9) (a) Muller, A.; Talbot, F.; Leutwyler, S. *J. Chem. Phys.* **2000**, *112*, 3717. (b) Smets, J.; Maes, G. *Chem. Phys. Lett.* **1991**, *187*, 532. (c) Florio, G. M.; Gruenloh, C. J.; Quimpo, R. C.; Zwier, T. S. *J. Chem. Phys.* **2000**, *113*, 11143. (d) Matsuda, Y.; Ebata, T.; Mikami, N. *J. Chem. Phys.* **1999**, *110*, 8397. (e) Matsuda, Y.; Ebata, T.; Mikami, N. *J. Chem. Phys.* **2000**, *113*, 573. (f) Held, A.; Pratt, D. W. *J. Am. Chem. Soc.* **1990**, *112*, 8629. (g) Held, A.; Pratt, D. W. *J. Am. Chem. Soc.* **1993**, *115*, 9708. (h) Held, A.; Pratt, D. W. *J. Chem. Phys.* **1992**, *96*, 4869. (i) Nimlos, M. R.; Kelley, D. F.; Bernstein, E. R. *J. Phys. Chem.* **1989**, *93*, 643. (j) Hatherley, L. D.; Brown, R. D.; Godfrey, P. D.; Pierlot, A. P. *J. Phys. Chem.* **1993**, *97*, 46.

(10) (a) Alkorta, I.; Elgureo, J. *J. Org. Chem.* **2002**, *67*, 1515. (b) Borst, D. R.; Roscioli, J. R.; Pratt, D. W.; Florio, G. M.; Zwier, T. S.; Muller, A.; Leutwyler, S. *Chem. Phys.* **2002**, *283*, 341. (c) Tautermann, C. S.; Voegele, A. F.; Liedl, K. R. *Chem. Phys.* **2003**, *292*, 47. (d) Muller, A.; Talbot, F.; Leutwyler, S. *J. Chem. Phys.* **2001**, *115*, 5192.

(11) Reimers, J. R.; Hall, L. E.; Hush, N. S. *J. Phys. Chem. A* **2000**, *104*, 5087.

(12) Becke, A. D. *J. Chem. Phys.* **1993**, *98*, 5648.

(13) Onsager, L. *J. Am. Chem. Soc.* **1938**, *58*, 1486.

(14) (a) Fukui, K. *J. Phys. Chem.* **1970**, *74*, 4161. (b) Gonzalez, C.; Schlegel, H. B. *J. Phys. Chem.* **1987**, *90*, 2154.

(15) GAUSSIAN 98, revision A.7, Frisch, M. J.; Trucks, G. W.; Schlegel, H. B.; Scuseria, G. E.; Robb, M. A.; Cheeseman, J. R.; Zakrzewski, V. G.; Montgomery, J. A., Jr., Stratmann, R. E.; Burant, J. C.; Dapprich, S.; Millam, J. M.; Daniels, A. D.; Kudin, K. N.; Strain, M. C.; Farkas, O.; Tomasi, J.; Barone, V.; Cossi, M.; Cammi, R.; Mennucci, B.; Pomelli, C.; Adamo, C.; Clifford, S.; Ochterski, J.; Petersson, G. A.; Ayala, P. Y.; Cui, Q.; Morokuma, K.; Malick, D. K.; Rabuck, A. D.; Raghavachari, K.; Foresman, J. B.; Cioslowski, J.; Ortiz, J. V.; Baboul, A. G.; Stefanov, B. B.; Liu, G.; Liashenko, A.; Piskorz, P.; Komaromi, I.; Gomperts, R.; Martin, R. L.; Fox, D. J.; Keith, T.; Al-Laham, M. A.; Peng, C. Y.; Nanayakkara, A.; Gonzalez, C.; Challacombe, M.; Gill, P. M. W.; Johnson, B.; Chen, W.; Wong, M. W.; Andres, J. L.; Gonzalez, C.; Head-Gordon, M.; Replogle, E. S.; Pople, J. A., Gaussian, Inc.: Pittsburgh, PA, 1998.

(16) The permanent dipole−dipole interaction energy, $U_{d-d}(r)$, is given below.

$$U_{d-d}(r) = -2\mu_1^2\mu_2^2/(4\pi\epsilon)^2(3K_BT) \times 1/r^6$$

McQuarrie, D. A.; Simon, J. D. *Physical Chemistry A Molecular Approach*, Chapter 16, University Science Books 1997.

$$U_{d-d}(r = 5\text{Å}) = -2 \times (3.4806 \times 3.3356 \times 10^{-30})^4/ [(3 \times 1.380658 \times 10^{-23} \times 300) \times (1.11265 \times 10^{-10})^2 \times (5 \times 10^{-10})^6]$$
$$= -1.5082 \times 10^{-20} \text{ Joule}$$
$$= -2.17 \text{ kcal/mol}$$

(17) The C2h-symmetry constrained TS geometry was determined and is shown in Figure S15 (Supporting Information). The optimized geometry has two imaginary frequencies ($\nu_1^{\ddagger} = 2008.94\text{i cm}^{-1}$, $\nu_2^{\ddagger} = 1449.42\text{i cm}^{-1}$) and is not of the real TS.